

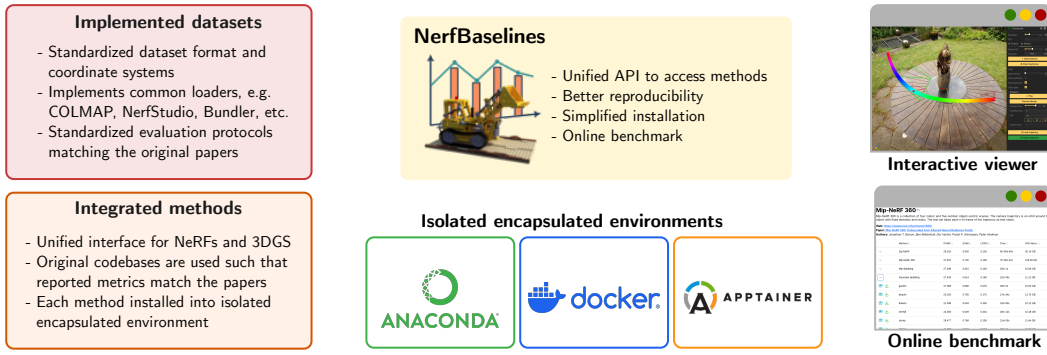
# NerfBaselines: Consistent and Reproducible Evaluation of Novel View Synthesis Methods

**Jonas Kulhanek**

CTU in Prague and ETH Zurich  
Czech Republic and Switzerland  
jonas.kulhanek@cvut.cz

**Torsten Sattler**

CTU in Prague  
Czech Republic  
torsten.sattler@cvut.cz



## Abstract

Novel view synthesis is an important problem with many applications, including AR/VR, gaming, and simulations for robotics. With the recent rapid development of Neural Radiance Fields (NeRFs) and 3D Gaussian Splatting (3DGS) methods, it is becoming difficult to keep track of the current state of the art (SoTA) due to methods using different evaluation protocols, codebases being difficult to install and use, and methods not generalizing well to novel 3D scenes. Our experiments support this claim by showing that tiny differences in evaluation protocols of various methods can lead to inconsistent reported metrics. To address these issues, we propose a framework called NerfBaselines, which simplifies the installation of various methods, provides consistent benchmarking tools, and ensures reproducibility. We validate our implementation experimentally by reproducing numbers reported in the original papers. To further improve the accessibility, we release a web platform where commonly used methods are compared on standard benchmarks.

**Web:** <https://jkulhanek.com/nerfbaselines>

## 1 Introduction

Due to the explosive growth in the number of NeRF-based and 3DGS-based works, with about 10 new papers citing NeRF [37] and 3 papers citing 3DGS [19] each day, there isn't a single evaluation framework and the individual works are based on different codebases for evaluation, resulting in numbers that sometimes are not directly comparable. Different methods sometimes use different evaluation protocols for the same datasets and often use specific data processing or hyperparameters which do not translate well to novel datasets (not used in the original papers). Furthermore, methods are often difficult to install with conflicting dependencies, and the codebases differ significantly,

which makes custom visualization or benchmarking laborious. To address these issues, we propose a framework designed to standardize and simplify the evaluation and comparison of these methods.

Not all papers follow the same evaluation protocol (partly because it is not fully specified) and sometimes innocuous changes can have a significant impact on the overall results. Examples include methods using different image resolutions for evaluation, different parameters for image downscaling, or different parameters for computing metrics. In our experiments, we show that even small discrepancies can cause substantial differences in the metrics, validating the need for a framework such as NerfBaselines. Our framework standardizes evaluation protocols, following best practices for each benchmark dataset.

Even with access to original source codes, reproducing paper results can be challenging due to codebases evolving over time or some codebases becoming obsolete where it is no longer possible to install the dependencies. To tackle this, for each method, we provide a consistent and reproducible way of installation (by encapsulating the runtime environment) which enables us to release checkpoint that can be used to render from custom camera positions without the need to rerun the training. Furthermore, we release a website with benchmarks comparing various methods on multiple datasets.

Many existing codebases cannot be easily applied to novel datasets due to having simplifying assumptions in the code, e.g., not implementing various camera models, requiring uniform camera intrinsic, or image sizes being equal. Various methods also use different interfaces, dataset formats, and coordinate systems, making integration and custom rendering laborious. Therefore, in NerfBaselines, we have integrated some important and influential codebases and implemented the missing functionality. Thankfully, most codebases are derived from the few original repositories (often with minor modifications), and therefore, they can also be integrated easily. Our experiments show that our integrated methods match the original ones with sufficient precision.

Furthermore, most methods compare using a set of metrics (e.g., PSNR) computed on a set of images taken as a subset of the training trajectory, which does not necessarily correlate well with the performance outside of the training trajectory [29]. Rendering videos from custom trajectories is often much better at demonstrating multiview consistency. Therefore, we release a web-based camera trajectory editor, based on Viser [53], to design camera trajectories and standardize their format. The common interface allows all integrated methods to render novel images from these trajectories.

In summary, to simplify benchmarking and improve reproducibility, we propose:

- A unified interface for NeRF and 3DGS methods, standardizing dataset formats and evaluation protocols.
- The NerfBaselines framework, which installs each method in an isolated environment to manage dependencies and ensure reproducibility. We experimentally verify our integrated methods reproduce results from original papers.
- A web-based camera trajectory editor and tools to render different camera trajectories, offering a more comprehensive assessment of performance beyond traditional metrics like PSNR, SSIM [6], or LPIPS [70].
- A web platform for comparing the performance of various methods on different datasets, providing checkpoints, and enabling interactive viewing of results.

## 2 Literature review

In recent years, progress in novel view synthesis has enabled real-time photo-realistic rendering of images from novel camera viewpoints. There has been a surge of interest, first with the advent of neural radiance field methods (NeRFs) [37, 30] which enabled photo-realistic results and a wide range of application. The second wave of attention came with the introduction of 3D Gaussian Splatting [19], matching NeRFs in terms of the rendering quality while enabling real-time rendering.

**Ray-based methods.** NeRFs represent a scene using a continuous volumetric radiance field, originally parameterized by a fully connected neural network [37, 2]. While this method enables high-quality rendering for forward-facing or bounded and object-centric scenes, it initially suffered from aliasing issues, which were addressed in [2] and extended to unbounded scenes in [3, 69]. However, the MLPs used in NeRFs posed a bottleneck in terms of both training and rendering speeds. To address this, caching of the radiance field was proposed to enable faster rendering [16, 45], though this came at the cost of large storage requirements. Consequently, several methods have investigated replacing MLPs

with alternatives such as *sparse grids* [14, 52], *point clouds* [61], *tetrahedral meshes* [24], *tensorial factorizations* [9, 15, 46], or *hash-grids* [39, 4, 56], often combined with tiny MLPs on top of the internal representation. While each approach has its advantages and disadvantages, hash-grids [39] have become the most popular representation due to their speed and scalability, with Zip-NeRF [4] achieving SoTA performance by addressing the aliasing issues of grid-based representations.

NeRFs have been extended in various ways, such as handling dynamic scenes [41, 44], modeling different image appearances [33, 15], and accommodating data with imprecise poses [5, 42]. They have also been applied to model semantics [21, 22] and for style transfer [54, 17]. To better model geometry, some methods replace the radiance field’s density with a signed distance function (SDF) [55, 57, 63]. Finally, another line of work focuses on extending these methods to generative [11, 43] or sparse-view settings [66, 8, 26], where the method is trained on a class of environments and then performs novel view synthesis given a few context images.

**Rasterization methods**, which project 3D geometry onto 2D image planes [19, 13], can be fast thanks to hardware optimization (rasterization pipelines have been dominant in the past). Recently, Gaussian Splatting (3DGS) [19] has gained popularity by matching the rendering quality of NeRFs while rendering at real-time speeds. 3DGS represents scenes using 3D Gaussians, which are projected onto the image plane [72], rasterized, and alpha-composited to render a view.

Like NeRFs, 3DGS has been modified to handle aliasing issues [67, 31], extended to larger scenes [20], and optimized to reduce the size of the representation [40] and to improve its geometric accuracy [18]. A minor change to the adaptive density control (ACD) was proposed in [65, 68] – where the sum of gradients was replaced with a sum of its norm , and a faster initialization method was proposed in [12]. Additionally, 3DGS has been applied to various domains, including SLAM [34] and physics simulation [59]. It has been extended to handle dynamic scenes [32] and semantics [71] using an N-D rasterizer. Generative 3DGS has also been proposed [10].

Unlike ray-based approaches which sample pixels randomly from training views, 3DGS optimizes on full images, requiring different training batch formation. In NerfBaselines, we do not enforce any specific way of constructing training batches, allowing each method to use the format it needs.

## 2.1 Existing codebases

Most current methods are based on a few core repositories: NerfStudio [53], Multi-NeRF [2, 3], Instant-NGP [39] for NeRFs, and Gaussian Splatting (INRIA) [19] for 3DGS, typically with moderate modifications. Therefore, in NerfBaselines, we focused on integrating these core repositories, as it simplifies the subsequent integration of derivative works. In Figure 1, we illustrate the relationships between popular repositories and highlight those currently integrated with NerfBaselines.

**NerfStudio** is a popular framework that introduced the modular separation of NeRFs into components such as ray samplers, radiance field heads, etc. It supports various dataloaders, camera types, and export formats. Unfortunately, the rapid evolution of NerfStudio introduces frequent breaking changes. Therefore, in NerfBaselines, we freeze each method to ensure reproducibility.

**Multi-NeRF** is fully implemented in JAX and does not have custom CUDA kernels (unlike Instant-NGP or NerfStudio), making it easy to install, but slower. Early versions based on Mip-NeRF360 supported only a single camera per dataset and a single image size; therefore, in NerfBaselines, we have extended these methods to handle more complex datasets.

**Instant-NGP** is a highly optimized implementation that has inspired numerous follow-up works [4, 53, 21, 22]. However, it is a less popular choice as a codebase due to its C++ training code being more difficult to extend. Since the repository

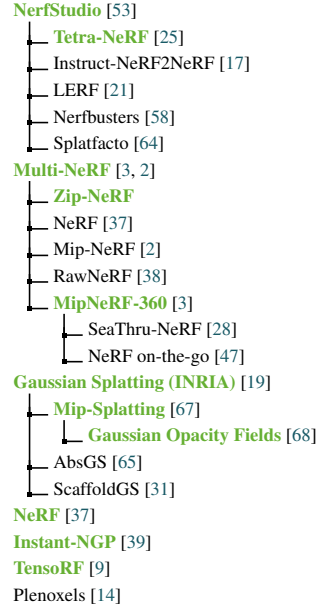


Figure 1: **Existing codebases.** Integrated methods are **bold green**.

does not natively support rendering with custom (distorted) cameras, in NerfBaselines, we have implemented this functionality.

**Gaussian Splatting (INRIA)** is the most popular choice for 3DGS methods, primarily because (until recently) it was unmatched in performance. The repository only supports pinhole cameras with their centre of projection being in center of the image. We have extended it to work with arbitrary camera models, performing undistortion/distortion for more complicated camera models.

### 3 Framework design

When designing the NerfBaselines framework, we aimed to address common issues when benchmarking novel view synthesis methods. These include: **different interfaces**, where each codebase has a different structure, making it difficult to interface with it. To this end, we propose a unified interface that all methods can share. **Installation challenges** arise as various methods often require specific and potentially difficult-to-install dependencies. To simplify the process, we install each method in a separate environment where we fully control the dependencies. For **fair evaluation**, we implement a standardized evaluation protocol for all methods, closely matching the original protocols proposed with the datasets. **Reproducibility** is ensured by carefully storing and tracking checkpoints used to generate predictions and compute metrics. Additionally, we have implemented a viewer with a trajectory editor and a public website to compare existing methods on standard benchmark datasets.

**Unified method API.** The different codebases [53, 3, 19, 9, 19] have very different code structures making it difficult to interface with them in a unified way. While studying the codebases, we identified a common structure which can be shared between all existing methods, regardless if they are raycasting-based (as in the case of NeRF codebases [53, 3, 19, 9, 60]), or rasterization-based (as in 3DGS methods [19, 20, 67, 68, 64]). For each codebase, we define a class called `method`, which encapsulates all that is needed to train the method and render new images from an existing checkpoint. Each method implements (among others) methods: `train_iteration` - which performs one training step, and `render` - which renders images from input cameras. Additionally, if the method supports appearance conditioning [33, 53], it implements the functionality to obtain the embeddings from unseen images. The detailed interface is given in the *supp. mat*.

**Environment isolation.** Installing methods is often difficult due to a set of hard-to-install and sometimes obsolete dependencies, e.g., CUDA, CuDNN, GCC, or OpenGL, where the version must match. The dependencies are sometimes in conflict with each other or in conflict with the user’s environment. Therefore, we provide a level of isolation, where each method is installed in its own isolated environment, allowing for different/conflicting dependencies without polluting the user’s environment. The user then communicates with the isolated environments using interprocess communication. NerfBaselines then handles the installation of all necessary dependencies the first time a user uses a method. We provide three levels of isolation: Anaconda [1], Docker [35], and Apptainer [27]: **1)** While Anaconda [1] is commonly used in research and is easy to install even on HPC clusters, it does not offer a good level of isolation, as some dependencies are inherited from the system, e.g., glibc, OpenGL, and, therefore, may fail on some systems. **2)** Docker [35] provides the best level of isolation, fully encapsulating the user environment (except for the CUDA drivers needed to control GPUs). Unfortunately, it is more difficult to install and is not commonly present on HPC clusters. Therefore, we also support the alternative **3)** Apptainer [27] with a better level of isolation than Anaconda that is more commonly present on HPC clusters.

**Unified dataloader.** Different codebases store and load data in various ways, complicating the process of integrating and evaluating methods across different datasets. For example, they use different downscaling algorithms and resolutions, different background colors, etc. The camera poses processing pipeline is also important, where methods like Instant-NGP [39] and NerfStudio [53] are sensitive to the scale of the scene, which depends on the camera placement relative to the scene’s geometry. We propose a unified interface for dataset loading and processing to address these issues and to facilitate the transfer to new datasets. We implement support for commonly used dataset formats such as COLMAP [49, 48], NeRF’s transforms.json [37], NerfStudio’s transforms.json [53], Bundler [51, 50] (also supported by RealityCapture [7]), NeRF in the Wild Photo Tourism [33, 50] splits format, Tanks and Temples [23], and the LLFF dataset format [36]. The loaders ensure consistent data processing and provide a uniform interface and camera format for all datasets, thereby simplifying integration and evaluation across diverse datasets. It also makes the development of new

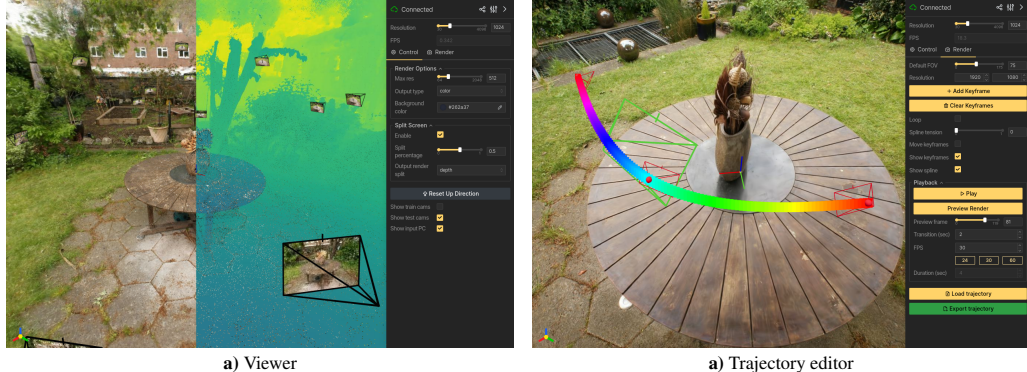


Figure 2: The **NerfBaselines Viewer** enables interactive rendering, shows train/test cameras, and input point cloud. It also has a trajectory editor (shown in the left figure).

methods easier as they do not need to implement their own dataloaders anymore. Furthermore, to simplify the ease of use, we support an automatic download of commonly used benchmark datasets such as the Blender dataset [37] and the Mip-NeRF 360 dataset [3].

**Viewer & camera trajectory rendering.** For novel view synthesis methods, evaluation is often conducted on a set of test images that are typically a subsequence of the training views. Unfortunately, this approach does not adequately demonstrate the method’s robustness and multiview consistency in capturing the 3D scene [29]. Rendering a video from a custom trajectory from truly novel viewpoints farther away from the training images provides a more insightful evaluation. While the unified interface presented in Section 3 ‘Unified method API’ significantly simplifies the process of rendering such trajectories, we further enhance this capability by providing an interactive viewer. This viewer allows users to inspect how the method performs outside the training camera distribution and includes a camera trajectory editor for designing custom trajectories. The viewer, based on NerfStudio’s viewer [53] and utilizing the Viser platform [53] for the web interface, is depicted in Figure 2, where the viewer interface is shown on the left and the trajectory editor on the right. The trajectory editor also enables exporting the trajectory in a format suitable for subsequent rendering.

**Fair evaluation & Reproducibility** Evaluating and comparing different methods is challenging because original codebases often use different evaluation protocols. For example, some methods use different parameters for SSIM [6] and different LPIPS [70] architectures (like AlexNet vs. VGG). Some methods even use different image resolutions [60, 62], or compute metrics on the raw image (float range) as opposed to rounding to the uint8 range – which cannot be reproduced from the commonly saved images. Therefore, we standardize the evaluation protocol by fixing the parameters of the metrics, resolution of images, and other aspects of the evaluation.

Sharing checkpoints often greatly improve research reproducibility, enabling validation of predicted test images and rendering 3D scenes from novel viewpoints. To enable this, NerfBaselines stores checkpoints to ensure models can be restored later. During method evaluation, we store the checkpoint SHA and verify it matches the released checkpoint. For all methods, we fix random seeds to match the official implementations. Additionally, for each integrated method, we provide a set of tests to confirm that loading the checkpoint genuinely reproduces the results.

**Web platform & Extensibility.** As part of the NerfBaselines toolbox, we release a website where methods are compared and their numbers (measured with NerfBaselines) reported. It also enables the checkpoints and the predictions to be downloaded for all scenes. The web can be found at <https://jkulhanek.com/nerfbaselines>.

Finally, NerfBaselines is designed in such that it makes it easy to extend it with new methods and datasets. Therefore we provide extension points to register new datasets, new evaluation protocols, and add new loggers (currently, we implement wandb and tensorboard loggers). The new method can be added by implementing the protocol described in Section 3 ‘Unified method API’ and providing a specification file, containing the installation script and method’s metadata.

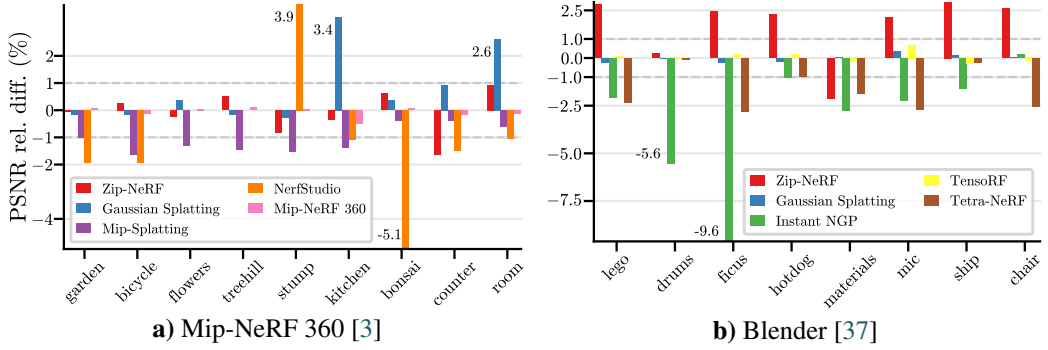


Figure 3: **Mip-NeRF 360 [3] and Blender [37] results** comparing PSNRs obtained via NerfBaselines with those reported in the original papers. We show the relative difference in %. In most cases, the difference is  $< 1\%$ . Instant-NGP [39] and Mip Splatting [67] are consistently underperforming because different evaluation protocols were used in the papers.

## 4 Evaluation

In our experiments, we **1)** verify that the integrated methods match the original metrics, **2)** show the tradeoff between quality and training cost, **3)** motivate the need for standardized evaluation protocols by demonstrating that small changes in evaluation protocol can bias results, **4)** demonstrate transferability to novel datasets, and **5)** qualitatively compare methods outside training trajectories. All our experiments used NVIDIA A100 GPUs. A single GPU was used for all but Mip-NeRF 360 [3], which used four GPUs. For comparisons, we use PSNR, SSIM [6], and LPIPS [70] (AlexNet). In the main paper, we mostly report PSNR, while other results can be found in the *supp. mat.*

### 4.1 Reproducing published results

First, to validate our framework, we reevaluate important methods on the standard benchmark datasets: Mip-NeRF 360 [3] and Blender [37]. We use the same evaluation protocol for all methods. The results are compared to the original numbers as published in the papers in Figure 3, with detailed numbers given in the *supp. mat.* Note, that in the figures and tables, we only compare with methods that released their numbers on the datasets in the corresponding publications.

**Mip-NeRF 360 results.** As shown in Figure 3, NerfBaselines reproduces the original results with a deviation of less than 1% for most scenes. For Mip-Splatting [67] and 3DGS [19], the difference in the numbers was caused by the different evaluation protocols used as discussed in Section 4.3. In the case of NerfStudio [53] and Tetra-NeRF [25], the codebase evolved since the time of the release which is likely the cause of the difference.

**Blender results.** From the results, the discrepancy is again small for most methods. However, for the Instant-NGP method [39], we can notice larger differences in PSNR, especially for ‘drums’, and ‘ficus’. Note, that Instant-NGP [39] uses a black background for training and evaluation. We run additional experiments confirming this to be the case of the difference in the metrics. Since Tetra-NeRF [25] uses NerfStudio [53] and the codebase evolved since the time of the release, we can notice a slight drop in the performance.

### 4.2 Quality vs. computational cost

When comparing methods, image quality is important, but we also need to consider the computational cost of training. Some methods perform better but require more computational power, while others achieve good results with less computation. To compare and visualize this, we plot the performance of different methods against their computational resources in Figure 4. We measure computational cost as the training time multiplied by GPU memory use. The reasoning is that most methods can be sped up with more GPU memory or larger batch sizes, while low GPU memory usage allows training on cheaper GPUs. We also show the variance in performance and computational cost. For both the Mip-NeRF 360 [3] and Blender [37] datasets, performance variance is similar across methods.

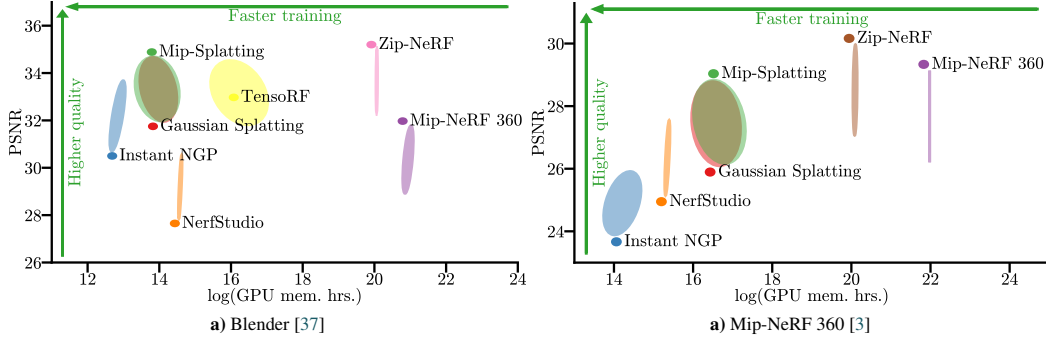


Figure 4: **Performance vs. training cost tradeoff.** We compare different methods’ rendering quality (PSNR↑) and rendering cost (GPU mem. hrs.↓). The variance across different scenes is visualized by the ellipse scale. While Zip-NeRF [4] performs the best, it is more costly to train than 3DGS[19].

	garden kitchen	bicycle bonsai	flowers counter	treehill room	stump
NerfStudio [53]	26.21/25.96/+0.96% 29.87/29.96/-0.28%	24.06/23.61/+1.90% 30.51/30.52/-0.02%	21.43/21.12/+1.45% 26.91/26.80/+0.43%	23.23/22.85/+1.66% 30.79/30.56/+0.76%	26.09/25.75/+1.33% 27.70/27.32/+1.37%
Zip-NeRF [4]	28.58/28.18/+1.40% 32.57/32.39/+0.55%	26.35/25.87/+1.85% 34.89/34.67/+0.64%	22.69/22.34/+1.56% 29.14/28.90/+0.82%	24.43/24.01/+1.73% 33.22/32.95/+0.80%	27.70/27.32/+1.37% 26.82/26.48/+1.29%
Gaussian Splatting [19]	27.75/27.37/+1.40% 31.65/31.36/+0.92%	25.62/25.20/+1.65% 32.29/32.10/+0.60%	21.84/21.60/+1.14% 28.97/28.97/+0.03%	22.75/22.46/+1.30% 31.38/31.43/-0.17%	26.82/26.48/+1.29%
Mip-Splatting [4]	27.85/27.48/+1.34% 31.55/31.12/+1.38%	25.68/25.30/+1.51% 32.39/32.18/+0.65%	21.93/21.64/+1.35% 29.07/29.04/+0.10%	22.99/22.64/+1.52% 31.68/31.55/+0.42%	26.88/26.52/+1.33%

Table 1: **Mip-NeRF 360 [3] image downscale protocol.** We compare the manual downscaling with the default protocol using released downscaled images (*middle number*). While NeRFs use released downscaled images, 3DGS-based methods [19] downscale images internally without compression. *Indoor scenes* and outdoor scenes have downscale factors of 2 and 4, respectively.

However, due to its adaptive nature, computational cost variance is much higher for methods based on Gaussian Splatting [19] compared to NeRF-based methods [37, 3, 4].

### 4.3 Mip-NeRF 360 evaluation protocol details

As stressed in the introduction, ensuring the same evaluation protocol is crucial in benchmarking. In this section, we demonstrate this by comparing two evaluation protocols that were used for the Mip-NeRF 360 dataset [3]. In Section 4.1, we have seen that NerfBaselines achieves consistently lower PSNR for Mip Splatting [67]. The reason is that while NeRFs train/evaluate on released downscaled images, the 3DGS [19] and Mip Splatting codebases [67] downscale from the large original images during training and evaluation (without storing them as JPEGs, thus avoiding compression artifacts). From the results presented in Table 1, we can see that while the difference is not large and the relative ordering is preserved, not using compression consistently gives results with larger PSNR. The difference is larger for outdoor scenes, where the downscale factor of 4 was used as opposed to indoor scenes with a downscale factor of 2.

### 4.4 Tanks & Temples evaluation

To demonstrate how NerfBaseline simplifies the transfer of existing methods to new datasets, we evaluate various integrated methods on the Tanks and Temples [23] dataset. For the dataset, we run COLMAP reconstruction [48, 49] with a simple radial camera model shared for all images. Afterward, we undistorted and downscaled images by a factor of 2. For NerfStudio [53], we run the Mip-NeRF 360 configuration (which from our experiments performs better on the dataset). The results are given in Table 2. As we can see the reconstructions are dominated by Zip-NeRF [4] for easier scenes, while for ‘Advanced’, there is no single best-performing method. We believe this is caused by NeRFs with its fixed capacity does not scale as well to larger scenes as 3DGS, where the capacity is adaptively increased.

PSNR↑	barn	caterpillar	truck	lighthouse	playground	train	auditorium	ballroom	courtroom	museum	palace	temple
	Training Data			Intermediate			Advanced					
Instant NGP [39]	25.90	21.72	22.85	21.65	23.33	20.01	20.67	21.62	19.44	15.19	19.09	17.84
NerfStudio [53]	26.40	21.71	23.37	20.85	24.69	20.43	20.77	22.68	20.24	17.84	17.68	17.06
Zip-NeRF [4]	29.26	23.94	25.09	23.07	27.13	22.19	24.52	25.45	22.17	19.34	19.11	20.58
Gaussian Splatting [19]	27.51	23.38	24.25	22.11	25.37	21.67	24.13	24.07	23.12	20.92	19.63	20.85
Mip-Splatting [67]	27.75	23.42	24.36	22.25	25.87	21.82	24.41	24.15	23.00	20.88	19.63	20.55
Gaussian Opacity Fields [68]	25.72	21.78	22.33	21.80	23.89	19.69	23.20	22.84	21.15	19.92	16.46	20.29
SSIM↑												
	0.772	0.633	0.770	0.765	0.696	0.657	0.761	0.652	0.640	0.471	0.668	0.689
	0.794	0.666	0.797	0.768	0.755	0.693	0.771	0.705	0.673	0.648	0.640	0.678
Instant NGP [39]	0.884	0.802	0.864	0.849	0.880	0.814	0.877	0.835	0.790	0.746	0.718	0.805
NerfStudio [53]	0.852	0.791	0.853	0.843	0.848	0.791	0.871	0.824	0.790	0.764	0.736	0.806
Zip-NeRF [4]	0.855	0.790	0.857	0.844	0.861	0.795	0.872	0.826	0.791	0.768	0.731	0.805
Gaussian Splatting [19]	0.866	0.791	0.860	0.833	0.869	0.796	0.871	0.818	0.781	0.761	0.683	0.794
LPIPS↑												
	0.271	0.360	0.216	0.281	0.343	0.334	0.429	0.352	0.448	0.606	0.440	0.424
	0.215	0.302	0.167	0.245	0.249	0.261	0.330	0.261	0.336	0.311	0.452	0.392
Instant NGP [39]	0.083	0.152	0.081	0.131	0.095	0.119	0.153	0.113	0.153	0.159	0.317	0.183
NerfStudio [53]	0.160	0.190	0.108	0.156	0.170	0.171	0.193	0.101	0.165	0.160	0.350	0.222
Zip-NeRF [4]	0.161	0.197	0.109	0.159	0.155	0.172	0.196	0.098	0.165	0.158	0.354	0.226
Gaussian Splatting [19]	0.140	0.187	0.099	0.181	0.142	0.164	0.194	0.107	0.168	0.152	0.443	0.234
Mip-Splatting [67]												
Gaussian Opacity Fields [68]												

Table 2: **Tanks & Temples [23] results.** We show the PSNR, SSIM [6], and LPIPS [70] (AlexNet) of various implemented methods. The first, second, and third values are highlighted.

#### 4.5 Off-trajectory qualitative comparison

While test-set metrics enable an effective way of comparing different methods, they are insufficient to fully evaluate the perceived quality [29]. Rendering images from poses with varying distances from the training camera’s trajectory provides a lot of insight into the robustness of the learned representations. Therefore, NerfBaselines provides a viewer and a renderer to enable visualising methods and rendering images/videos outside the train trajectory. In Figure 5, we compare various methods by rendering trained scenes both close to the training camera trajectory and far from it. Notice how in the second row Instant-NGP [39], and 3DGS methods [19, 67] cannot fill the sparsely observed sky, while NerfStudio [53] and Zip-NeRF [4] can achieve it thanks to space contraction. Also, notice how 3DGS methods [19, 67] are more blurred in less observed regions.

### 5 Conclusion

In conclusion, our NerfBaselines framework addresses the major challenges in evaluating novel view synthesis methods, e.g. NeRFs and 3DGS. By standardizing evaluation protocols and designing a unified interface, we enable fair comparisons and scalability to novel datasets. The camera trajectory editor enables multiview consistency evaluation, while the NerfBaselines framework ensures smooth installation and reproducibility by using isolated environments. Additionally, our web platform displays benchmark results, comparing various methods across different datasets. The NerfBaselines framework thus improves the fairness and effectiveness of novel view synthesis method evaluations.

**License.** This project is released under the **MIT** license. The integrated methods may be licensed under various licenses, and it is the user’s responsibility to conform to the conditions before using a method. Note that while NerfBaselines enables access to various methods, the user still uses the original official codebases (with some wrapper code to interface with it).

**Limitations.** While NerfBaselines offers consistent and reproducible benchmarking, it requires methods to expose the same interface either directly or by writing a wrapper script. While we integrated some well-known methods and will gradually add more, our hope is that the scientific community could collaborate and adopt the interface for future methods.

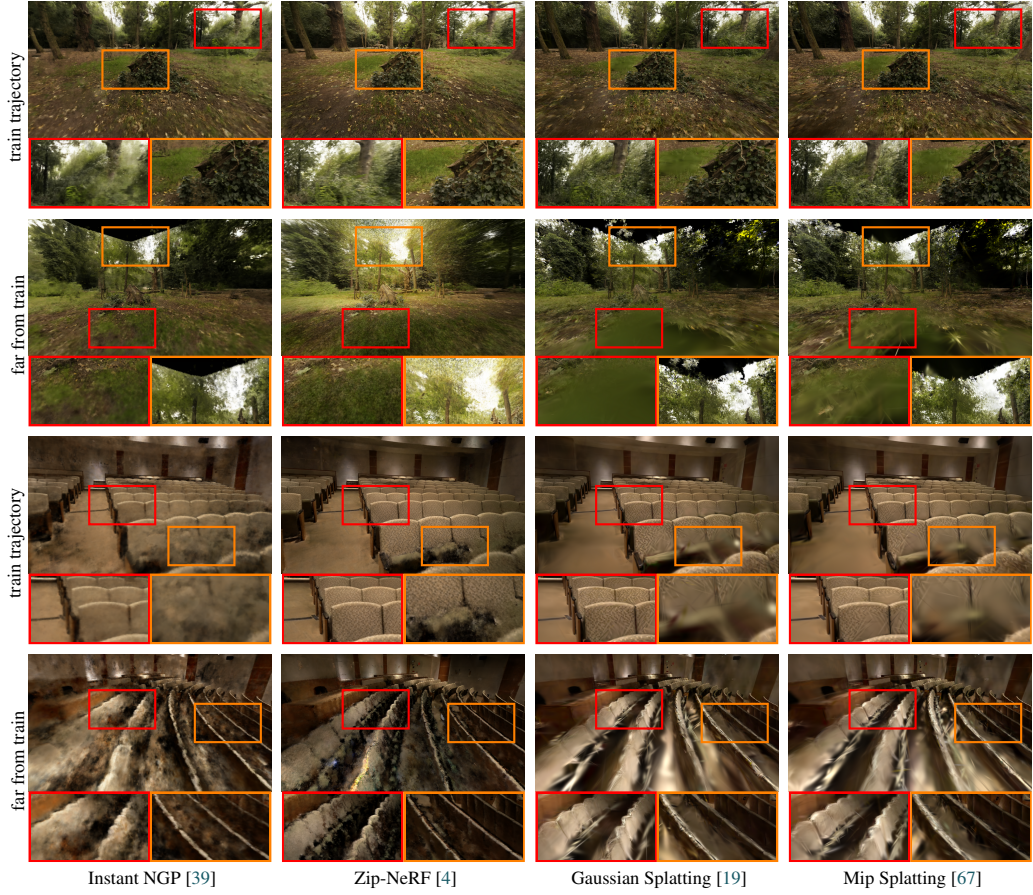


Figure 5: **Qualitative results.** We compare methods on views close and far from the training trajectory. **Top:** MipNeRF360/stump scene, **bottom:** T&T/Auditorium.

**Broader impact.** While training and evaluating all methods require significant computational resources and associated carbon emissions, our release of reproducible checkpoints minimizes the need for repeated training by other researchers, thereby reducing overall environmental impact.

## Acknowledgments and Disclosure of Funding

We want to thank Brent Yi and the NerfStudio Team for helpful discussions regarding the NerfStudio codebase and for releasing the Viser platform. This work was supported by the Czech Science Foundation (GAČR) EXPRO (grant no. 23-07973X), the Grant Agency of the Czech Technical University in Prague (grant no. SGS24/095/OHK3/2T/13), and by the Ministry of Education, Youth and Sports of the Czech Republic through the e-INFRA CZ (ID:90254)

## References

- [1] Anaconda. Anaconda software distribution, 2020. URL <https://docs.anaconda.com/>. 4
- [2] Jonathan T Barron, Ben Mildenhall, Matthew Tancik, Peter Hedman, Ricardo Martin-Brualla, and Pratul P Srinivasan. Mip-nerf: A multiscale representation for anti-aliasing neural radiance fields. In *ICCV*, pages 5855–5864, 2021. 2, 3
- [3] Jonathan T Barron, Ben Mildenhall, Dor Verbin, Pratul P Srinivasan, and Peter Hedman. Mip-nerf 360: Unbounded anti-aliased neural radiance fields. In *CVPR*, 2022. 2, 3, 4, 5, 6, 7, 14, 16

- [4] Jonathan T Barron, Ben Mildenhall, Dor Verbin, Pratul P Srinivasan, and Peter Hedman. Zip-nerf: Anti-aliased grid-based neural radiance fields. In *ICCV*, pages 19697–19705, 2023. 3, 7, 8, 9, 14, 15, 16
- [5] Wenjing Bian, Zirui Wang, Kejie Li, Jia-Wang Bian, and Victor Adrian Prisacariu. Nope-nerf: Optimising neural radiance field with no pose prior. In *CVPR*, pages 4160–4169, 2023. 3
- [6] Dominique Brunet, Edward R. Vrscay, and Zhou Wang. On the mathematical properties of the structural similarity index. *IEEE TIP*, 2012. 2, 5, 6, 8
- [7] Capturing Reality. Reality capture 1.4, 2024. URL <https://www.capturingreality.com/>. Software. 4
- [8] Anpei Chen, Zexiang Xu, Fuqiang Zhao, Xiaoshuai Zhang, Fanbo Xiang, Jingyi Yu, and Hao Su. Mvsnerf: Fast generalizable radiance field reconstruction from multi-view stereo. In *ICCV*, pages 14124–14133, 2021. 3
- [9] Anpei Chen, Zexiang Xu, Andreas Geiger, Jingyi Yu, and Hao Su. TensoRF: Tensorial radiance fields. In *ECCV*, 2022. 3, 4, 15
- [10] Yuedong Chen, Haofei Xu, Chuanxia Zheng, Bohan Zhuang, Marc Pollefeys, Andreas Geiger, Tat-Jen Cham, and Jianfei Cai. Mvsplat: Efficient 3d gaussian splatting from sparse multi-view images. *arXiv*, 2024. 3
- [11] Congyue Deng, Chiyu Jiang, Charles R Qi, Xinchen Yan, Yin Zhou, Leonidas Guibas, Dragomir Anguelov, et al. Nerdi: Single-view nerf synthesis with language-guided diffusion as general image priors. In *CVPR*, pages 20637–20647, 2023. 3
- [12] Zhiwen Fan, Wenyang Cong, Kairun Wen, Kevin Wang, Jian Zhang, Xinghao Ding, Danfei Xu, Boris Ivanovic, Marco Pavone, Georgios Pavlakos, Zhangyang Wang, and Yue Wang. InstantSplat: Unbounded sparse-view pose-free gaussian splatting in 40 seconds. *arXiv*, 2024. 3
- [13] Linus Franke, Darius Rückert, Laura Fink, and Marc Stamminger. Trips: Trilinear point splatting for real-time radiance field rendering. *CGF*, 43(2), 2024. doi: <https://doi.org/10.1111/cgf.15012>. 3
- [14] Sara Fridovich-Keil, Alex Yu, Matthew Tancik, Qinhong Chen, Benjamin Recht, and Angjoo Kanazawa. Plenoxels: Radiance fields without neural networks. In *CVPR*, pages 5501–5510, 2022. 3
- [15] Sara Fridovich-Keil, Giacomo Meanti, Frederik Rahbæk Warburg, Benjamin Recht, and Angjoo Kanazawa. K-planes: Explicit radiance fields in space, time, and appearance. In *CVPR*, 2023. 3
- [16] Stephan J Garbin, Marek Kowalski, Matthew Johnson, Jamie Shotton, and Julien Valentin. Fastnerf: High-fidelity neural rendering at 200fps. In *ICCV*, pages 14346–14355, 2021. 2
- [17] Ayaan Haque, Matthew Tancik, Alexei Efros, Aleksander Holynski, and Angjoo Kanazawa. Instruct-nerf2nerf: Editing 3d scenes with instructions. In *ICCV*, 2023. 3
- [18] Binbin Huang, Zehao Yu, Anpei Chen, Andreas Geiger, and Shenghua Gao. 2D gaussian splatting for geometrically accurate radiance fields. *arXiv*, 2024. 3
- [19] Bernhard Kerbl, Georgios Kopanas, Thomas Leimkühler, and George Drettakis. 3d gaussian splatting for real-time radiance field rendering. *ACM TOG*, 2023. 1, 2, 3, 4, 6, 7, 8, 9, 14, 15, 16
- [20] Bernhard Kerbl, Andreas Meuleman, Georgios Kopanas, Michael Wimmer, Alexandre Lanvin, and George Drettakis. A hierarchical 3d gaussian representation for real-time rendering of very large datasets. *ACM TOG*, 43(4), July 2024. 3, 4
- [21] Justin Kerr, Chung Min Kim, Ken Goldberg, Angjoo Kanazawa, and Matthew Tancik. Lerf: Language embedded radiance fields. In *ICCV*, pages 19729–19739, 2023. 3
- [22] Chung Min Kim, Mingxuan Wu, Justin Kerr, Ken Goldberg, Matthew Tancik, and Angjoo Kanazawa. Garfield: Group anything with radiance fields. *arXiv*, 2024. 3
- [23] Arno Knapitsch, Jaesik Park, Qian-Yi Zhou, and Vladlen Koltun. Tanks and temples: Benchmarking large-scale scene reconstruction. *ACM TOG*, 36(4), 2017. 4, 7, 8, 14
- [24] Jonas Kulhanek and Torsten Sattler. Tetra-nerf: Representing neural radiance fields using tetrahedra. In *ICCV*, 2023. 3
- [25] Jonas Kulhanek and Torsten Sattler. Tetra-nerf: Representing neural radiance fields using tetrahedra. In *ICCV*, pages 18458–18469, 2023. 3, 6, 15

- [26] Jonáš Kulhánek, Erik Derner, Torsten Sattler, and Robert Babuška. Viewformer: Nerf-free neural rendering from few images using transformers. In *ECCV*, pages 198–216. Springer, 2022. 3
- [27] Gregory M. Kurtzer, cclerget, Michael Bauer, Ian Kaneshiro, David Trudgian, and David Godlove. hpcng/singularity: Singularity 3.7.3, 2021. 4
- [28] Deborah Levy, Amit Peleg, Naama Pearl, Dan Rosenbaum, Derya Akkaynak, Simon Korman, and Tali Treibitz. Seathru-nerf: Neural radiance fields in scattering media. In *CVPR*, pages 56–65, 2023. 3
- [29] Hanxue Liang, Tianhao Wu, Param Hanji, Francesco Banterle, Hongyun Gao, Rafal Mantiuk, and Cengiz Oztireli. Perceptual quality assessment of nerf and neural view synthesis methods for front-facing views. In *Eurographics*, 2023. 2, 5, 8
- [30] Stephen Lombardi, Tomas Simon, Jason Saragih, Gabriel Schwartz, Andreas Lehrmann, and Yaser Sheikh. Neural volumes: learning dynamic renderable volumes from images. *ACM TOG*, 38(4):1–14, 2019. 2
- [31] Tao Lu, Mulin Yu, Lining Xu, Yuanbo Xiangli, Limin Wang, Dahua Lin, and Bo Dai. Scaffold-GS: Structured 3D gaussians for view-adaptive rendering. *arXiv*, 2023. 3
- [32] Jonathon Luiten, Georgios Kopanas, Bastian Leibe, and Deva Ramanan. Dynamic 3d gaussians: Tracking by persistent dynamic view synthesis. In *3DV*, 2024. 3
- [33] Ricardo Martin-Brualla, Noha Radwan, Mehdi SM Sajjadi, Jonathan T Barron, Alexey Dosovitskiy, and Daniel Duckworth. Nerf in the wild: Neural radiance fields for unconstrained photo collections. In *CVPR*, 2021. 3, 4
- [34] Hidenobu Matsuki, Riku Murai, Paul H. J. Kelly, and Andrew J. Davison. Gaussian Splatting SLAM. *CVPR*, 2024. 3
- [35] Dirk Merkel. Docker: lightweight linux containers for consistent development and deployment. *Linux journal*, 2014(239):2, 2014. 4
- [36] Ben Mildenhall, Pratul P Srinivasan, Rodrigo Ortiz-Cayon, Nima Khademi Kalantari, Ravi Ramamoorthi, Ren Ng, and Abhishek Kar. Local light field fusion: Practical view synthesis with prescriptive sampling guidelines. *ACM TOG*, 38(4), 2019. 4
- [37] Ben Mildenhall, Pratul P Srinivasan, Matthew Tancik, Jonathan T Barron, Ravi Ramamoorthi, and Ren Ng. NeRF: Representing scenes as neural radiance fields for view synthesis. In *ECCV*, 2020. 1, 2, 3, 4, 5, 6, 7, 14
- [38] Ben Mildenhall, Peter Hedman, Ricardo Martin-Brualla, Pratul P Srinivasan, and Jonathan T Barron. Nerf in the dark: High dynamic range view synthesis from noisy raw images. In *CVPR*, pages 16190–16199, 2022. 3
- [39] Thomas Müller, Alex Evans, Christoph Schied, and Alexander Keller. Instant neural graphics primitives with a multiresolution hash encoding. *ACM TOG*, 2022. 3, 4, 6, 8, 9, 14, 15
- [40] Panagiotis Papantonakis, Georgios Kopanas, Bernhard Kerbl, Alexandre Lanvin, and George Drettakis. Reducing the memory footprint of 3d gaussian splatting. *ACM CGIT*, 2024. 3
- [41] Keunhong Park, Utkarsh Sinha, Jonathan T Barron, Sofien Bouaziz, Dan B Goldman, Steven M Seitz, and Ricardo Martin-Brualla. Nerfies: Deformable neural radiance fields. In *ICCV*, pages 5865–5874, 2021. 3
- [42] Keunhong Park, Philipp Henzler, Ben Mildenhall, Jonathan T Barron, and Ricardo Martin-Brualla. CamP: Camera preconditioning for neural radiance fields. *ACM TOG*, 42(6):1–11, 2023. 3
- [43] Ben Poole, Ajay Jain, Jonathan T Barron, and Ben Mildenhall. Dreamfusion: Text-to-3d using 2d diffusion. In *ICLR*, 2022. 3
- [44] Albert Pumarola, Enric Corona, Gerard Pons-Moll, and Francesc Moreno-Noguer. D-NeRF: Neural Radiance Fields for Dynamic Scenes. In *CVPR*, 2020. 3
- [45] Christian Reiser, Songyou Peng, Yiyi Liao, and Andreas Geiger. Kilonerf: Speeding up neural radiance fields with thousands of tiny mlps. In *ICCV*, pages 14335–14345, 2021. 2
- [46] Christian Reiser, Rick Szeliski, Dor Verbin, Pratul Srinivasan, Ben Mildenhall, Andreas Geiger, Jon Barron, and Peter Hedman. Merf: Memory-efficient radiance fields for real-time view synthesis in unbounded scenes. *ACM TOG*, 42(4):1–12, 2023. 3

- [47] Weining Ren, Zihan Zhu, Boyang Sun, Jiaqi Chen, Marc Pollefeys, and Songyou Peng. Nerf on-the-go: Exploiting uncertainty for distractor-free nerfs in the wild. In *CVPR*, 2024. 3
- [48] Johannes Lutz Schönberger and Jan-Michael Frahm. Structure-from-motion revisited. In *CVPR*, 2016. 4, 7
- [49] Johannes Lutz Schönberger, Enliang Zheng, Marc Pollefeys, and Jan-Michael Frahm. Pixelwise view selection for unstructured multi-view stereo. In *ECCV*, 2016. 4, 7
- [50] Noah Snavely, Steven M Seitz, and Richard Szeliski. Photo tourism: exploring photo collections in 3d. *ACM TOG*, 2006. 4
- [51] Noah Snavely, Steven M Seitz, and Richard Szeliski. Modeling the world from internet photo collections. *IJCV*, 80:189–210, 2008. 4
- [52] Cheng Sun, Min Sun, and Hwann-Tzong Chen. Direct voxel grid optimization: Super-fast convergence for radiance fields reconstruction. In *CVPR*, 2022. 3
- [53] Matthew Tancik, Ethan Weber, Evonne Ng, Rui long Li, Brent Yi, Terrance Wang, Alexander Kristoffersen, Jake Austin, Kamyar Salahi, Abhik Ahuja, et al. Nerfstudio: A modular framework for neural radiance field development. In *ACM TOG*, 2023. 2, 3, 4, 5, 6, 7, 8, 14, 16
- [54] Can Wang, Ruixiang Jiang, Menglei Chai, Mingming He, Dongdong Chen, and Jing Liao. Nerf-art: Text-driven neural radiance fields stylization. *IEEE TVCG*, 2023. 3
- [55] Peng Wang, Lingjie Liu, Yuan Liu, Christian Theobalt, Taku Komura, and Wenping Wang. Neus: Learning neural implicit surfaces by volume rendering for multi-view reconstruction. *NeurIPS*, 34:27171–27183, 2021. 3
- [56] Peng Wang, Yuan Liu, Zhaoxi Chen, Lingjie Liu, Ziwei Liu, Taku Komura, Christian Theobalt, and Wenping Wang. F2-nerf: Fast neural radiance field training with free camera trajectories. In *CVPR*, pages 4150–4159, 2023. 3
- [57] Yiming Wang, Qin Han, Marc Habermann, Kostas Daniilidis, Christian Theobalt, and Lingjie Liu. Neus2: Fast learning of neural implicit surfaces for multi-view reconstruction. In *ICCV*, pages 3295–3306, 2023. 3
- [58] Frederik Warburg, Ethan Weber, Matthew Tancik, Aleksander Holynski, and Angjoo Kanazawa. Nerf-busters: Removing ghostly artifacts from casually captured nerfs. In *ICCV*, pages 18120–18130, 2023. 3
- [59] Tianyi Xie, Zeshun Zong, Yuxin Qiu, Xuan Li, Yutao Feng, Yin Yang, and Chenfanfu Jiang. Physgaussian: Physics-integrated 3d gaussians for generative dynamics. *arXiv*, 2023. 3
- [60] Qiangeng Xu, Zexiang Xu, Julien Philip, Sai Bi, Zhixin Shu, Kalyan Sunkavalli, and Ulrich Neumann. Point-nerf: Point-based neural radiance fields. In *CVPR*, pages 5438–5448, 2022. 4, 5
- [61] Qiangeng Xu, Zexiang Xu, Julien Philip, Sai Bi, Zhixin Shu, Kalyan Sunkavalli, and Ulrich Neumann. Point-nerf: Point-based neural radiance fields. In *CVPR*, pages 5438–5448, 2022. 3
- [62] Yifan Yang, Shuhai Zhang, Zixiong Huang, Yubing Zhang, and Mingkui Tan. Cross-ray neural radiance fields for novel-view synthesis from unconstrained image collections. In *ICCV*, 2023. 5
- [63] Lior Yariv, Jiatao Gu, Yoni Kasten, and Yaron Lipman. Volume rendering of neural implicit surfaces. *NeurIPS*, 34:4805–4815, 2021. 3
- [64] Vickie Ye, Matias Turkulainen, and the Nerfstudio team. gsplat, 2024. URL <https://github.com/nerfstudio-project/gsplat>. 3, 4
- [65] Zongxin Ye, Wenyu Li, Sidun Liu, Peng Qiao, and Yong Dou. Absgs: Recovering fine details for 3d gaussian splatting. *arXiv*, 2024. 3
- [66] Alex Yu, Vickie Ye, Matthew Tancik, and Angjoo Kanazawa. pixelnerf: Neural radiance fields from one or few images. In *CVPR*, pages 4578–4587, 2021. 3
- [67] Zehao Yu, Anpei Chen, Binbin Huang, Torsten Sattler, and Andreas Geiger. Mip-splatting: Alias-free 3d gaussian splatting. In *CVPR*, 2024. 3, 4, 6, 7, 8, 9, 14, 16
- [68] Zehao Yu, Torsten Sattler, and Andreas Geiger. Gaussian opacity fields: Efficient high-quality compact surface reconstruction in unbounded scenes. *arXiv*, 2024. 3, 4, 8

- [69] Kai Zhang, Gernot Riegler, Noah Snavely, and Vladlen Koltun. Nerf++: Analyzing and improving neural radiance fields. *arXiv*, 2020. [2](#)
- [70] Richard Zhang, Phillip Isola, Alexei A Efros, Eli Shechtman, and Oliver Wang. The unreasonable effectiveness of deep features as a perceptual metric. In *CVPR*, 2018. [2](#), [5](#), [6](#), [8](#), [14](#)
- [71] Shijie Zhou, Haoran Chang, Sicheng Jiang, Zhiwen Fan, Zehao Zhu, Dejia Xu, Pradyumna Chari, Suya You, Zhangyang Wang, and Achuta Kadambi. Feature 3dgs: Supercharging 3d gaussian splatting to enable distilled feature fields. *CVPR*, 2024. [3](#)
- [72] Matthias Zwicker, Hanspeter Pfister, Jeroen Van Baar, and Markus Gross. Surface splatting. In *ACM TOG*, 2001. [3](#)

---

# Supplementary Material

---

## NerfBaselines: Consistent and Reproducible Evaluation of Novel View Synthesis Methods

---

In the Supplementary Material, we extend Section 3 from the main paper by providing the full Method API in Appendix A.1. We describe the video released as part of the Supplementary Material (at <https://jkulhanek.com/nerfbaselines/video>) in Appendix A.2. We extend the reproducibility comparison from Section 4 of the main paper in Appendix A.3. We show screenshots of the web platform in Appendix A.4. We give the instructions on how to use NerfBaselines and reproduce the results in Appendix A.5. Finally, we provide detailed licenses for integrated methods in Appendix A.6.

### A.1 Method API

Every method implements the following interface:

- `constructor(train_dataset?, checkpoint?)`: The constructor takes as its inputs the (optional) training dataset instance (a set of images and camera parameters) or the (optional) checkpoint. At least one of the two has to be provided.
- `train_iteration`: Performs one training step (using the train dataset), updating the parameters.
- `save(path)`: Saves the current checkpoint.
- `render(cameras, embeddings?)`: Renders the 3D scene using the list of camera parameters with an optional list of camera embeddings if the method supports appearance conditioning.
- `get_info` and `get_method_info`: Returns information about the trained model and the base method, respectively.
- (optional) `optimize_embeddings(dataset)`: Optimizes the appearance embeddings on the dataset (if the method supports it).

### A.2 Video

In the attached video (at <https://jkulhanek.com/nerfbaselines/video>), we compare Gaussian Splatting [19], Mip-Splatting [67], Zip-NeRF [4], Instant-NGP [39], and NerfStudio [53]. We generate trajectories such that we start from regions close to the training trajectory, then we move further from the scene center and close to geometry to visualize how different methods handle these viewpoint changes. We show the results on two scenes from the Mip-NeRF 360 dataset [3] (stump and kitchen), and two scenes from the Tanks and Temples dataset [23] (temple and lighthouse). Notice, how 3DGS behaves well close to the training trajectory but has blank spots outside (where the geometry is missing). On the other hand, NeRFs (especially NerfStudio [53]) is better able to extrapolate to less visible regions further from the scene center.

### A.3 Reproducing paper results

To extend the data reported in the main paper, we further give the detailed PSNR and SSIM scores for Blender [37] and Mip-NeRF 360 [3] datasets. From the results, we can see that SSIM behaves similarly to PSNR with mostly smaller differences (except for the Tetra-NeRF run on the Blender/ship scene). However, LPIPS (VGG) [70] numbers are very different from the papers. There are two reasons: **1)** Multi-NeRF [3] and 3DGS [19] codebases both have a bug in LPIPS computation, where

the images which should be normalized to  $[-1, 1]$  range is kept in the  $[0, 1]$  range. This makes the errors smaller. If we also change our evaluation not to normalize to  $[-1, 1]$ , we reproduce their results. Since these codebases are the basis for most other methods, the bug is shared for other methods as well. **2)** A smaller reason present in the case of NerfStudio is that we evaluate all metrics on images in the `uint8` range (to be reproducible from the stored image). While this change does not have much influence on PSNR and SSIM, LPIPS is more sensitive to these changes.

## A.4 Web platform

To keep track of the current state of the art (SoTA), we release a web platform (<https://jkulhanek.com/nerfbaselines>). The web platform shows results on all individual scenes for all methods, enables comparing methods, and allows users to download checkpoints and predictions for the datasets. Example screenshots can be seen in Figure 6.

## A.5 Use instructions

**Installation.** Before installing NerfBaselines, Python 3.7+ must be installed on the host system. We recommend using either `conda` or `venv` to separate NerfBaselines from system packages. After

PSNR ↑	lego materials	drums mic	ficus ship	hotdog chair
Instant NGP [39]	35.64/36.39/-2.05% 28.95/29.78/-2.77%	24.57/26.02/-5.55% 35.40/36.22/-2.25%	30.29/33.51/-9.62% 30.60/31.70/-1.62%	37.01/37.40/-1.03% 35.06/35.00/+0.17%
TensoRF [9]	36.49/36.46/+0.09% 30.08/30.12/-0.14%	26.01/26.01/-0.00% 34.85/34.61/+0.68%	34.06/33.99/+0.19% 30.69/30.77/-0.26%	37.49/37.41/+0.20% 35.72/35.76/-0.11%
Tetra-NeRF [25]	33.93/34.75/-2.36% 28.75/29.30/-1.88%	24.99/25.01/-0.09% 34.54/35.49/-2.68%	32.37/33.31/-2.82% 31.06/31.13/-0.22%	35.80/36.16/-0.98% 34.17/35.05/-2.52%
Zip-NeRF [4]	35.81/34.84/+2.79% 30.98/31.66/-2.15%	25.90/25.84/+0.23% 35.90/35.15/+2.14%	34.73/33.90/+2.44% 32.30/31.38/+2.94%	37.98/37.14/+2.27% 35.75/34.84/+2.62%
Gaussian Splatting [19]	35.70/35.78/-0.24% 30.01/30.00/+0.02%	26.15/26.15/-0.01% 35.49/35.36/+0.36%	34.79/34.87/-0.22% 30.85/30.80/+0.15%	37.64/37.72/-0.21% 35.84/35.83/+0.04%
SSIM ↑	lego materials	drums mic	ficus ship	hotdog chair
Instant NGP [39]	0.981/-/ 0.944/-/	0.930/-/ 0.989/-/	0.972/-/ 0.892/-/	0.982/-/ 0.984/-/
TensoRF [9]	0.983/0.983/+0.01% 0.952/0.952/+0.04%	0.936/0.937/-0.05% 0.988/0.988/+0.03%	0.982/0.982/+0.04% 0.894/0.895/-0.14%	0.982/0.982/+0.04% 0.984/0.985/-0.06%
Tetra-NeRF [25]	0.972/0.987/-1.57% 0.941/0.968/-2.77%	0.927/0.947/-2.08% 0.987/0.993/-0.60%	0.977/0.989/-1.22% 0.896/0.994/-9.83%	0.978/0.989/-1.09% 0.977/0.990/-1.35%
Zip-NeRF [4]	0.983/0.980/+0.29% 0.967/0.969/-0.19%	0.948/0.944/+0.38% 0.992/0.991/+0.11%	0.987/0.985/+0.19% 0.937/0.929/+0.83%	0.987/0.984/+0.25% 0.987/0.983/+0.36%
Gaussian Splatting [19]	0.982/-/ 0.959/-/	0.953/-/ 0.991/-/	0.987/-/ 0.904/-/	0.985/-/ 0.987/-/
LPIPS <sub>VGG</sub> ↓	lego materials	drums mic	ficus ship	hotdog chair
Instant NGP [39]	0.020/-/ 0.069/-/	0.109/-/ 0.016/-/	0.031/-/ 0.136/-/	0.037/-/ 0.023/-/
TensoRF [9]	0.022/0.018/+23.33% 0.059/0.058/+1.31%	0.076/0.073/+4.16% 0.021/0.015/+39.93%	0.029/0.022/+30.50% 0.141/0.138/+2.44%	0.033/0.032/+2.16% 0.027/0.022/+22.86%
Tetra-NeRF [25]	0.036/-/ 0.076/-/	0.087/-/ 0.022/-/	0.032/-/ 0.129/-/	0.040/-/ 0.029/-/
Zip-NeRF [4]	0.019/0.019/-6.63% 0.040/0.032/+26.50%	0.054/0.050/+8.08% 0.008/0.007/+16.14%	0.014/0.015/-6.00% 0.114/0.091/+24.84%	0.023/0.020/+12.70% 0.017/0.017/+0.24%
Gaussian Splatting [19]	0.019/-/ 0.043/-/	0.044/-/ 0.008/-/	0.013/-/ 0.130/-/	0.026/-/ 0.015/-/

Table 3: **Blender results comparing PSNR, SSIM, and LPIPS (VGG) obtained via NerfBaselines with those reported in the original papers.** We show the current PSNR/original PSNR/relative difference in %. The darker the color, the larger the difference. The differences for Instant NGP [39] are larger because the paper used a black background (instead of the default white). For LPIPS (VGG), the differences are larger because the compared codebases do not normalize input images to the correct range.

PSNR ↑	garden kitchen	bicycle bonsai	flowers counter	treehill room	stump
Mip-NeRF 360 [3]	27.00/26.98/+0.07% 32.08/32.23/-0.48%	24.34/24.37/-0.12% 33.48/33.46/+0.05%	21.74/21.73/+0.04% 29.51/29.55/-0.15%	22.89/22.87/+0.10% 31.58/31.63/-0.14%	26.41/26.40/+0.04%
NerfStudio [53]	25.96/26.47/-1.91% 29.96/30.29/-1.10%	23.61/24.08/-1.94% 30.52/32.16/-5.11%	21.12/-/ 26.80/27.20/-1.48%	22.85/-/ 30.56/30.89/-1.06%	25.75/24.78/+3.91%
Zip-NeRF [4]	28.18/28.20/-0.05% 32.39/32.50/-0.34%	25.87/25.80/+0.26% 34.67/34.46/+0.61%	22.34/22.40/-0.25% 28.90/29.38/-1.63%	24.01/23.89/+0.51% 32.95/32.65/+0.93%	27.32/27.55/-0.82%
Gaussian Splatting [19]	27.37/27.41/-0.16% 31.36/30.32/+3.43%	25.20/25.25/-0.17% 32.10/31.98/+0.36%	21.60/21.52/+0.36% 28.97/28.70/+0.93%	22.46/22.49/-0.15% 31.43/30.63/+2.62%	26.48/26.55/-0.28%
Mip-Splatting [67]	27.48/27.76/-1.02% 31.12/31.55/-1.36%	25.30/25.72/-1.64% 32.18/32.31/-0.39%	21.64/21.93/-1.31% 29.04/29.16/-0.39%	22.64/22.98/-1.47% 31.55/31.74/-0.60%	26.52/26.94/-1.54%
SSIM ↑	garden kitchen	bicycle bonsai	flowers counter	treehill room	stump
Mip-NeRF 360 [3]	0.813/0.813/+0.01% 0.919/0.920/-0.11%	0.688/0.685/+0.41% 0.940/0.941/-0.08%	0.583/0.583/-0.01% 0.893/0.894/-0.09%	0.632/0.632/-0.08% 0.912/0.913/-0.07%	0.747/0.744/+0.37%
NerfStudio [53]	0.756/0.774/-2.28% 0.881/0.890/-0.96%	0.567/0.599/-5.34% 0.909/0.933/-2.61%	0.512/-/ 0.829/0.843/-1.66%	0.546/-/ 0.880/0.896/-1.82%	0.694/0.662/+4.90%
Zip-NeRF [4]	0.863/0.860/+0.37% 0.929/0.928/+0.14%	0.775/0.769/+0.78% 0.951/0.949/+0.24%	0.637/0.642/-0.80% 0.904/0.902/+0.21%	0.675/0.681/-0.93% 0.927/0.925/+0.24%	0.789/0.800/-1.35%
Gaussian Splatting [19]	0.866/0.868/-0.17% 0.927/0.922/+0.52%	0.765/0.771/-0.79% 0.941/0.938/+0.30%	0.604/0.605/-0.23% 0.907/0.905/+0.25%	0.629/0.638/-1.34% 0.917/0.914/+0.31%	0.768/0.775/-0.87%
Mip-Splatting [67]	0.869/0.875/-0.71% 0.927/0.933/-0.68%	0.766/0.780/-1.74% 0.941/0.948/-0.71%	0.604/0.623/-3.01% 0.907/0.916/-0.94%	0.635/0.655/-3.11% 0.917/0.928/-1.14%	0.770/0.786/-2.04%
LPIPS <sub>VGG</sub> ↓	garden kitchen	bicycle bonsai	flowers counter	treehill room	stump
Mip-NeRF 360 [3]	0.190/0.170/+11.59% 0.155/0.127/+22.06%	0.328/0.301/+9.10% 0.211/0.176/+19.82%	0.370/0.344/+7.63% 0.253/0.204/+24.18%	0.379/0.339/+11.93% 0.267/0.211/+26.38%	0.300/0.261/+14.76%
NerfStudio [53]	0.249/0.235/+5.95% 0.200/0.190/+5.03%	0.454/0.422/+7.46% 0.249/0.197/+26.27%	0.434/-/ 0.338/0.314/+7.71%	0.492/-/ 0.314/0.296/+5.98%	0.350/0.380/-8.01%
Zip-NeRF [4]	0.127/0.118/+7.85% 0.133/0.116/+15.07%	0.227/0.208/+8.91% 0.195/0.173/+12.77%	0.310/0.273/+13.41% 0.224/0.185/+20.83%	0.281/0.242/+16.11% 0.237/0.196/+20.88%	0.234/0.193/+21.44%
Gaussian Splatting [19]	0.123/0.103/+19.23% 0.155/0.129/+19.93%	0.239/0.205/+16.66% 0.253/0.205/+23.48%	0.366/0.336/+8.88% 0.257/0.204/+26.01%	0.379/0.317/+19.41% 0.286/0.220/+30.19%	0.251/0.210/+19.66%
Mip-Splatting [67]	0.124/0.103/+20.72% 0.155/0.113/+37.07%	0.241/0.206/+17.12% 0.253/0.173/+46.24%	0.371/0.331/+12.19% 0.258/0.179/+43.87%	0.379/0.320/+18.37% 0.286/0.192/+48.85%	0.253/0.209/+21.18%

Table 4: **Mip-NeRF 360** results comparing PSNR, SSIM, and LPIPS (VGG) obtained via **NerfBaselines** with those reported in the original papers. We show the current PSNR/original PSNR/relative difference in %. The darker the color, the larger the difference. For PSNR and SSIM, in most cases, the difference is < 1%. For LPIPS (VGG), the differences are larger because the compared codebases (except for NerfStudio) do not normalize input images to the correct range.

#### Mip-NeRF 360 ↗

Mip-NeRF 360 is a collection of four indoor and five outdoor object-centric scenes. The camera trajectory is an orbit around the object with fixed elevation and radius. The test set takes each n-th frame of the trajectory as test views.

Web: <https://jonbaron.info/minerf360/>

Paper: [Mip-NeRF 360: An Inlined Anti-aliased Neural Radiance Fields](#)

Authors: Jonathan T. Barron, Ben Mildenhall, Dor Verbin, Pratul P. Srinivasan, Peter Hedman

Method ↴	PSNR ↴	SSIM ↴	LPIPS <sub>VGG</sub> ↴	Time ↴	GPU Mem. ↴
Zip-NeRF	28.516	0.828	0.138	5h 30m 49s	26.19 GB
Mip-NeRF 360	27.670	0.792	0.196	7h 29m 42s	126.99 GB
Mip-Splatting	27.498	0.815	0.183	25m 1s	10.96 GB
Gaussian Splatting	27.439	0.814	0.180	22m 45s	11.12 GB
garden	27.366	0.866	0.076	28m 5s	15.64 GB
nerf++	29.261	0.794	0.174	97m 44s	1x 72.64

a) Dataset results view

#### Zip-NeRF ↗

Zip-NeRF is a radiance field method which addresses the aliasing problem in the case of hash-grid based methods (ING-based). Instead of sampling along the ray it samples along a spiral path - approximating integration along the frustum.

Web: <https://jonbaron.info/zonerf/>

Paper: [Zip-NeRF: Anti-Aliased Grid-Based Neural Radiance Fields](#)

Authors: Jonathan T. Barron, Ben Mildenhall, Dor Verbin, Pratul P. Srinivasan, Peter Hedman

#### Mip-NeRF 360 ↗

Mip-NeRF 360 is a collection of four indoor and five outdoor object-centric scenes. The camera trajectory is an orbit around the object with fixed elevation and radius. The test set takes each n-th frame of the trajectory as test views.

Scene ↴	PSNR ↴	SSIM ↴	LPIPS <sub>VGG</sub> ↴	Time ↴	GPU Mem. ↴
average	28.516	0.828	0.138	5h 30m 49s	26.19 GB

Blender

a) Method results view

Figure 6: **Web platform.** Shows the ranking of the current set of integrated methods. It enables downloading of the checkpoints and predictions, and for some methods, it provides an online viewer.

Python is ready, install the `nerfbaselines` pip package on your host system by running: `pip install nerfbaselines`. Now, `nerfbaselines` cli can be used to interact with NerfBaselines. However, at least one supported backend must be installed before any method can be used. At the moment there are the following backends implemented:

- **docker**: Offers good isolation, requires docker (with NVIDIA container toolkit) to be installed and the user to have access to it (being in the docker user group). In order to install it, please follow the instructions at <https://github.com/NVIDIA/nvidia-container-toolkit>
- **apptainer**: Similar level of isolation as docker, but does not require the user to have privileged access. To install the backend, please follow instructions at <https://apptainer.org/docs/admin/main/installation.html>.
- **conda** (default): Does not require docker/apptainer to be installed, but does not offer the same level of isolation and some methods require additional dependencies to be installed. Also, some methods are not implemented for this backend because they rely on dependencies not found on conda. To install conda, we recommend following instructions at <https://github.com/conda-forge/miniforge> to install the miniforge distribution of conda.
- **python**: Will run everything directly in the current environment. Everything needs to be installed in the environment for this backend to work.

Additionally, all backends require NVIDIA GPU drivers to be installed to access the GPUs. For NerfBaselines commands, the backend can be set either via the `--backend <backend>` argument or using the `NERFBASELINES_BACKEND` environment variable.

**Training.** To start the training, use the following command: `nerfbaselines train --method <method> --data external://<dataset>/<scene>`, where `<method>` can be e.g., `nerfacto`, `zipnerf`, `instant-ngp`, ... (for the full list, run `nerfbaselines train --help`). The `<dataset>` can be one of the following: `mipnerf360`, `blender`, `tanksandtemples`. Similarly, `<scene>` is the scene name in lowercase. The training script will automatically download the dataset and start the training. The training will also run the evaluation and output the metrics computed on the test set.

**Other commands.** The resulting checkpoint can be used in the viewer (`nerfbaselines viewer --checkpoint <checkpoint> --data external://<dataset>/<scene>`), to rerun the rendering (`nerfbaselines render --checkpoint <checkpoint> --data external://<dataset>/<scene>`), or to render a camera trajectory (`nerfbaselines render-trajectory --checkpoint <checkpoint> --trajectory <trajectory> --output <output>.mp4`). The full list of available command can be seen by running `nerfbaselines --help`.

## A.6 License

The NerfBaselines project is licensed under the [MIT license](#). Each implemented method is licensed under the license provided by the authors of the method. For the currently implemented methods, the following licenses apply:

- NerfStudio: [Apache 2.0](#)
- Instant-NGP: [custom, research purposes only](#)
- Gaussian-Splatting: [custom, research purposes only](#)
- Mip-Splatting: [custom, research purposes only](#)
- Gaussian Opacity Fields: [custom, research purposes only](#)
- Tetra-NeRF: [MIT, Apache 2.0](#)
- Mip-NeRF 360: [Apache 2.0](#)
- Zip-NeRF: [Apache 2.0](#)
- CamP: [Apache 2.0](#)